Astron. Astrophys. 347, 494–499 (1999)

ASTRONOMY AND ASTROPHYSICS

An atmospheric model for the ion cyclotron line of Geminga

A. Jacchia[1], **F. De Luca**[1,2], **E. Lazzaro**[1], **P.A. Caraveo**[3,4], **R.P. Mignani**[5], **and G.F. Bignami**[6,7]

[1] Istituto di Fisica del Plasma "P. Caldirola", CNR, Via Cozzi 53, I-20125 Milan, Italy (jacchia@ifp.mi.cnr.it)
[2] Universitá degli studi di Milano, Dipartimento di Fisica, Via Celoria 16, I-20133 Milan, Italy
[3] Istituto di Fisica Cosmica "G. Occhialini", CNR, Via Bassini 15, I-20133 Milan, Italy
[4] Istituto Astronomico, Via Lancisi 29, I-00161 Rome, Italy
[5] STECF-ESO, Karl-Schwarzschild-Strasse 2, D-85740 Garching, Germany
[6] Agenzia Spaziale Italiana, Via di Villa Patrizi 13, I-00161 Rome, Italy
[7] Universitá di Pavia, Via Bassi 6, I-27100 Pavia, Italy

Received 29 October 1998 / Accepted 29 April 1999

Abstract. Recent optical/UV data of Geminga (Mignani et al. 1998) have strengthen the significance of the emission feature present over the thermal continuum best fitting the EUV/soft X-ray data. Here we present a phenomenological model interpreting the data in terms of an ion cyclotron feature, arising from a thin outer layer of hot plasma covering Geminga's polar caps. The width of the feature favours for Geminga the strongly oblique rotator configuration, as already deduced from the soft X-ray data (Halpern & Ruderman 1993). Our interpretation implies a magnetic field of 3–5 10^{11} G, consistent with the value deduced from the dynamical parameters of the pulsar. This would represent the first case of an independent measurement of the surface magnetic field of an isolated neutron star.

The expected time modulation of Geminga's feature is also discussed.

Key words: radiation mechanisms: thermal – stars: pulsars: individual: Geminga = 1E 0630+1

1. Introduction

The panorama of optical observations of Isolated Neutron Stars (INS) is limited by the faintness of the vast majority of them. Only one object, the Crab pulsar, has good, medium resolution optical (Nasuti et al. 1996) and near-UV spectral data (Gull et al. 1998), while for PSR0540-69 the synchrotron continuum has been measured by HST (Hill et al. 1997). For a few more cases acceptable multicolour photometry exists, while the rest of the data base (a grand total of less than 10 objects currently) consists of one/two - wavelengths detections (see Caraveo 1998 for a summary of the observational panorama).

Apart from the very young objects, characterized by flat, synchrotron-like spectra arising from energetic electron interactions in their magnetosphere, of particular interest are the middle-aged ones ($\sim 10^5\ yrs$ old). The non-thermal, magnetospheric emission should have faded enough (in the X-ray waveband at least) to render visible the thermal emission from the hot INS surface. Standard cooling calculations predict a surface temperature in the range $10^5 - 10^6\ ^\circ K$, in excellent agreement with recent X-ray observations of INS with thermal spectra (e.g. Becker & Trümper 1997). It is easy to predict the IR-optical-UV fluxes generated along the $\sim E^2$ Rayleigh-Jeans slope of the Planck curve best fitting the X-ray data, and to compare predictions to observations, where available.

In what follows, we shall concentrate on Geminga, which is certainly the most studied object of its class (Bignami & Caraveo 1996 and refs. therein), and possibly of all INSs (except for the Crab). Its IR-optical-UV data (Bignami et al. 1996; Mignani et al. 1998) show the presence of a well defined emission feature. Such a feature is superimposed on the thermal continuum expected from the extrapolation of the black-body X-ray emission detected by ROSAT (e.g. Halpern & Ruderman 1993). The presence of a clear maximum centered on V has been recently questioned by Martin et al. (1998) on the basis of a spectrum which is at the limit of the capability of the Keck telescope. The spectrum of Geminga, detected at a level of just 0.5% of the dark sky, seems fairly flat and, although broadly consistent with earlier measurements, it is definitely above the flux measured in the B-band by the HST/FOC (Mignani et al. 1998). Therefore, in view of the faintness of the target, we shall concentrate on the photometric measurements, which have been repeated using different instrumental set-ups and appear more reliable than the available spectral data.

Recently, pulsations in the B-band have been tentatively detected by Shearer et al. (1998). Also in this case, the faintness of the source limits quite severely the S/N ratio and thus the statistical significance of the result. Indeed, a pulsed signal at just the 3.5 σ level was found during only one of the three nights devoted to the project. If confirmed, these measurements would have deep implications on the mechanisms responsible for the optical emission of Geminga. However, in view of the rather low statistical significance of these results, we shall stand by the interpretation of Mignani et al. (1998) and propose a phenomenological model interpreting the feature as an atmospheric cyclotron line emission from Geminga's polar caps.

Send offprint requests to: A. Jacchia

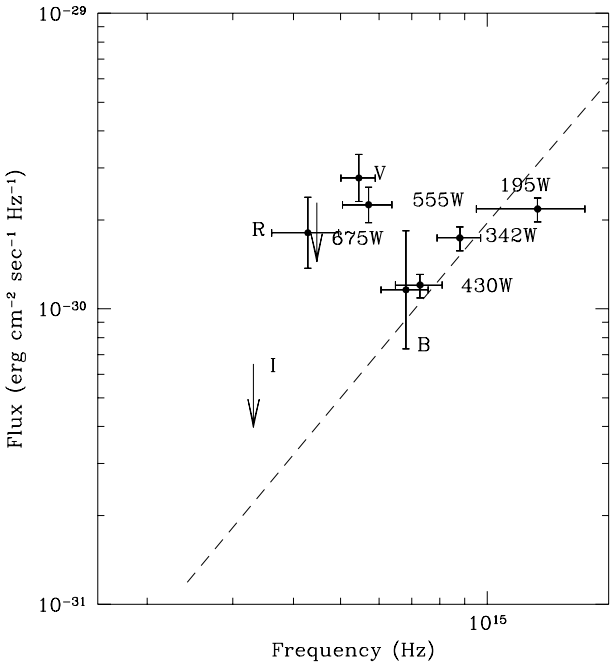

Fig. 1. The plot summarizes the complete multiband HST and ground-based photometry of Geminga. Three digits identify WFPC2/FOC imaging filters. The dashed line represents the extrapolation in the optical of the blackbody fit to the ROSAT data (Halpern & Ruderman 1993), which, for the best fitting temperature of $T = 5.77\ 10^5\ ^\circ K$ and the measured distance $d \simeq 157\ pc$ (Caraveo et al. 1996), yield an emitting radius $R = 10\ km$.

2. The spectral distribution

Fig. 1 shows the complete I-to-near UV colours of Geminga. These were obtained both from the ground and from HST during ten years of continuing observational effort (from Mignani et al. 1998). Comparing the repeteadly confirmed V-band magnitude with the relative fluxes of the three FOC points (430W, 342W and 195W) in the B/UV and the upper limit in I, it is easy to recognize an emission feature superimposed to a $\sim E^2$ RJ-like continuum. It is thus obvious to directly compare the measured optical fluxes to the extrapolation of the soft X-ray blackbody spectrum. However, this apparently trivial step is easier said than done, since different X-ray observations have yielded for Geminga slightly different best fitting temperatures, with significantly different bolometric fluxes. For example, two independent ROSAT observations yielded best fitting temperatures of $5.77\ 10^5\ ^\circ K$ (Halpern & Ruderman 1993) and $4.5\ 10^5\ ^\circ K$ (Halpern & Wang 1997), respectively, implying, for the same Geminga distance, a factor of 3 difference in the emitting area. As a reference, we show in Fig. 1 the Rayleigh-Jeans extrapolation of the ROSAT X-ray spectrum obtained using the best fitting temperature derived by Halpern & Ruderman (1993) which, at the Geminga distance (Caraveo et al. 1996), yields an emission radius of 10 km. Thus, while the optical, RJ-like, continuum is largely consistent with thermal emission from the neutron star surface, the feature around $\sim 6,000$ Å, requires a different interpretation.

In the following, we propose a phenomenological model interpreting the feature seen in Fig. 1 as an atmospheric cyclotron line emission from Geminga's polar caps.

3. The ion cyclotron emission model

Comparisons between theory and observed cooling NS spectra have been performed, e.g., by Romani (1987) and Meyer et al. (1994). Basically, the star surface is thought to be surrounded by a colder, partially ionized, atmosphere. Such an atmosphere behaves as a broad-band, absorbing-emitting medium. The observed spectrum is due to a rather complicate process, involving transfer of radiating energy between regions of different depths, temperatures and chemical compositions. These models predict a deviation from the blackbody emission law marginally observed in cooling neutron star spectra. Models that account for the effects of the star magnetic field B foresee absorption lines at the cyclotron frequencies. This is easily explained by the presence of resonant frequencies, created by the magnetic field, at which the radiation emitted from deeper regions is quite efficiently absorbed. On the other hand, a cyclotron emission "line", superimposed to the blackbody continuum, requires a thermal inversion of the stellar atmosphere. We will see in the following that a thin hot plasma layer is optically thick at the cyclotron frequency, so that the cyclotron emission is far more efficient than Bremsstrahlung in the same spectral range. For reasonable value of the plasma density, therefore, Bremsstrahlung can be neglected. Geminga's emission "line" might then be explained as an (ion) cyclotron emission from a magnetoplasma, consisting of a mixture of Hydrogen and Helium, surrounding the star surface. Any feature of the observed radiation spectrum of Geminga in the region of the proton cyclotron frequency is ultimately due to the accelerated motion of charged particles in the magnetic and electric fields of the rotating star. We assume, however, the upper part of the star atmosphere to be a fully ionized "classical" plasma layer, with a Maxwellian ion distribution function. The plasma layer is immersed in the inhomogeneous star dipole magnetic field. Accordingly, we develop the theory of the emission under the condition of applicability of the Kirchhoff's law. To this end it is necessary to consider the full dielectric response of the magnetized plasma, and address two key questions: (i) identification of an electromagnetic (e.m.) wave which can propagate in vacuo toward the observer and assessment of its thermal (black body) absorption/emission properties in a single or multiple species plasma, (ii) assessment of the emission line broadening mechanism as a consequence of Doppler effect, collisions, temperature and density inhomogeneity and averaging over the magnetic field.

3.1. The electromagnetic wave and its absorption/emission properties

If a medium emits radiation at a given frequency, it also absorbs it at the same frequency. The quantity $I(\omega)$, i.e. the radiated power per unit area per unit solid angle per unit angular frequency, is given by the solution of the radiative transfer equation.

For a single propagating e.m. mode in a medium of refractive index n this is written as:

$$n^2 \frac{d}{ds}\left(\frac{I(\omega)}{n^2}\right) = j(\omega) - \alpha(\omega) I(\omega) \quad (1)$$

where $j(\omega)$ and $\alpha(\omega)$ are the emissivity and the absorption coefficient respectively and s is the axis along the radiation path. In the present problem only one normal e.m. mode can propagate in vacuo and be observed. The emissivity, $j(\omega)$, is computed from the plasma dispersion relation and the Kirchhoff's law:

$$j(\omega) = \alpha(\omega) K(\omega, T) \quad (2)$$

where $K(\omega, T)$ is the Planck function at the temperature T, where T is here the plasma temperature. Near the cyclotron frequency ω_{ci} ($2\pi\,\nu_{ci} = \omega_{ci} = ZeB/Ac$; Z is the atomic charge A the atomic mass), two independent e.m. modes can propagate in the magnetized plasma atmosphere. They are identified by an index of refraction given by the complex roots $n_\pm = n' + i\,n''$ of the complex dispersion relation written for a real frequency $\omega \simeq \omega_{ci}$ in the biquadratic form (Akhiezer et al. 1975):

$$A n_\pm^4 + B n_\pm^2 + C = 0 \quad (3)$$

The coefficients A, B and C are functions of the full dielectric tensor and depend on the plasma frequency ω_p, the ion cyclotron frequency ω_{ci}, the ion temperature T_i and the angle θ between the propagation wave vector $\boldsymbol{k} = \frac{\omega}{c}\boldsymbol{n}$ and the local magnetic field $\boldsymbol{B}$. Of these two waves, the slow n_+ (ordinary) wave diverges at the cyclotron resonance with a finite bandwidth (roughly given by the ratio of the thermal velocity to the phase velocity) of anomalous dispersion around the cyclotron frequency.

The ordinary wave in the region where $\omega > \omega_{ci}$ has an evanescence gap, which even if bridging by thermal and collisional effects is considered, produces substantial attenuation of wave propagating in tenuous plasma toward the observer (Shafranov 1958, Akhiezer et al. 1975). The Geminga plasma atmosphere is characterized by $\omega_p/\omega_{ci} < 1$. This prevents the use of the customary ion cyclotron approximation of the dielectric tensor and a numerical solution of the dispersion relation for both the ordinary and extraordinary mode has been performed. The numerical evaluation of absorption and propagation properties of the mode propagating in vacuo are shown in Fig. 2. as function of the angle between the direction of propagation and the magnetic field. The extraordinary mode, which can propagate in vacuo with frequency $\omega \geq \omega_{ci}$, is the so called magnetosonic, compressional Alfven or fast wave.

It has a regular index of refraction and a very narrow band of frequency of anomalous dispersion with a correspondingly narrow frequency range of absorption due to thermal effects (Akhiezer et al., l975). The fast wave is electromagnetic in nature and in the cold plasma limit it is righthanded polarized. It becomes lefthanded (i.e. in the direction of the ion motion), thus allowing absorption at the fundamental harmonic, owing to small thermal effects or to the presence in the plasma of small traces of isotopes of the minority species. The Geminga plasma is characterized by $\omega_p/\omega_{ci} < 1$. This prevents the use of the

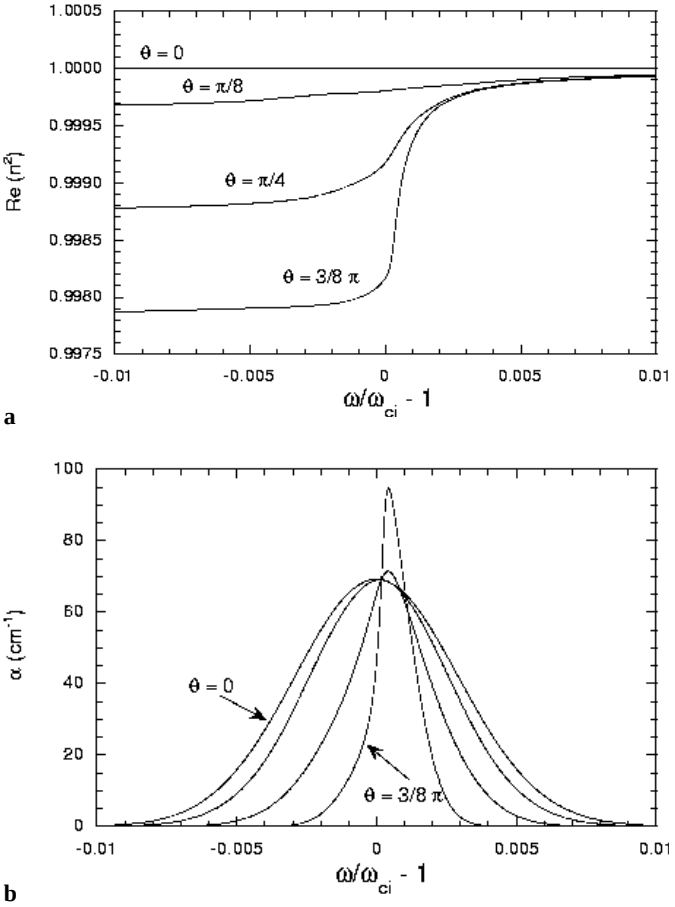

Fig. 2. a Plot of the real part of the square of refractive index $n^2(\omega, \theta)$ of the fast wave vs $\omega/\omega_{ci} - 1$ (where ω_{ci} is the ion cyclotron frequency), for different values of the angle θ between the direction of propagation and the magnetic field. Propagation toward the observer, on the "low field side" $\omega/\omega_{ci} \geq 1$ is guaranteed by the fact that n^2 is positive. **b** Plot of the absorption coefficient $\alpha(\omega, \theta)[cm^{-1}]$ of the fast wave vs $\omega/\omega_{ci} - 1$, for different values of the angle θ between the direction of propagation and the magnetic field. Calculation is done for a Hydrogen Maxwellian plasma with $B = 3.8\ 10^{11}\ G$, $n = 10^{19}[cm^{-3}]$, $T_i(\beta = 0^\circ) = 9\ 10^7\ ^\circ K$ (where T_i is the ion temperature) and it shows that optical thickness is obtained for plasma layer of the order of 1 cm at all propagation angles.

customary ion cyclotron approximation of the dielectric tensor and requires a numerical solution of the dispersion relation. Assuming an appropriate temperature and density, even in a pure H^+ plasma the fast wave reaches a sufficiently large absorption coefficient $\alpha(\omega, \theta) = 2\ (\omega/c)\ n''(\omega, \theta)$. The optical depth, τ, can be estimated as

$$\tau(\omega, \theta) = \int_0^L \alpha(\omega, \theta) ds' \simeq \alpha(\omega, \theta) L \gg 1 \quad (4)$$

where L is the plasma layer thickness, of the order of few cm. The refraction index of the fast wave and its absorption coefficient α are given in Fig. 2a,b for different θ angles, a plasma density of $10^{19} cm^3$ and a plasma temperature of $9\ 10^7\ ^\circ K$. It is worth noticing that, owing to the weak dependence of α on θ (see Fig. 2b), a layer of thickness less than 1 cm is sufficient

to match the blackbody emission, independently of the angle of propagation with respect to the magnetic field at any point on the star surface. We will use this condition to greatly simplify the computation of the intensity and of the broadening of the emitted line.

The intensity, $i(\omega, \omega_c)$, radiated from any point of the star surface, is then simply given by

$$i(\omega, \omega_{ci}) = K(T, \omega)[1 - e^{-\tau(\omega, \omega_{ci})}] \quad (5)$$

A density limit of about 10^{19} particles cm^{-3} represents an upper limit to the plasma density. Above such limit, bremsstrahlung, with its absorption coefficient $\alpha \simeq 10^{-2}(cm^{-1})$ (Bekefi 1966) in the range of temperature frequency of interest here, would introduce severe spectral distortions, not observed in the data.

Blackbody emission conditions could be met in a lower density region of the outer part of the atmosphere, with a slightly larger plasma thickness. This, however, would not change the main issue of the present model: the observed Geminga spectral feature comes from a plasma which belongs to the star atmosphere. One may alternatively think that the cyclotron line was emitted by the low density matter surrounding the star. This would imply that what is observed depends upon a process of photon collection over a wide plasma volume and, consequently, over a wide range of cyclotron frequencies. However, this is contradicted by the comparatively well defined peak now observed.

3.2. Emission line broadening mechanism

The real part of $n^2(\omega, \theta)$ shown in Fig. 2 exhibits a very narrow frequency band of anomalous dispersion. This indicates that the width of the observed emission line cannot be explained in terms of the thermal Doppler broadening ($\Delta\omega \simeq \omega|ncos\theta|\frac{v_{thi}}{c}$, where v_{thi} is the ion thermal velocity). This is by far insufficient to fit the observations in the range of temperatures required to explain the intensity of the line. Another possible source of broadening are collisional effects. These, however, have been shown to be insufficient to account for the width of the cyclotron feature. The only mechanism left to account for such an observed width is the structure of a dipole-like magnetic field associated with the star. In the case of a perfect magnetic dipole located at the centre of the star, the intensity of the magnetic field increases by a factor two when moving on the star surface from the (magnetic) equator to the poles. As a consequence, the ion cyclotron frequency should also change by a factor two, if the emitting plasma were to cover the whole star surface. The shape of the emission line is then determined by the superposition of radiation emitted by regions of the star with different magnetic field values and possibly different plasma temperature. The intensity of the line in our model is obtained as the integral of the emission from each point of the star surface:

$$I(\omega) = \frac{1}{D^2}\int_{\Sigma} i(\omega, \omega_{ci})\frac{\boldsymbol{n} \bullet \boldsymbol{k}}{|\boldsymbol{k}|}d^2\Sigma \quad (6)$$

where D is the distance of the star from the observer and the integral is extended to the whole surface, Σ, taking into account the usual geometry effects ($\boldsymbol{n}$ represents the unit vector perpendicular to $d^2\Sigma$, while $\boldsymbol{k}$ is the propagation vector pointing toward the observer). The non-homogeneous emission also depends on the relative position of the observer with respect to the star rotation axis and, to properly account for the shape and the intensity of the feature, on the angle γ between the rotation and magnetic axis. The computed spectrum, of course, will be averaged over the star rotation period. These model assumptions also allow us to determine the modulation depth expected for the observed spectral feature, yielding a clear observational test.

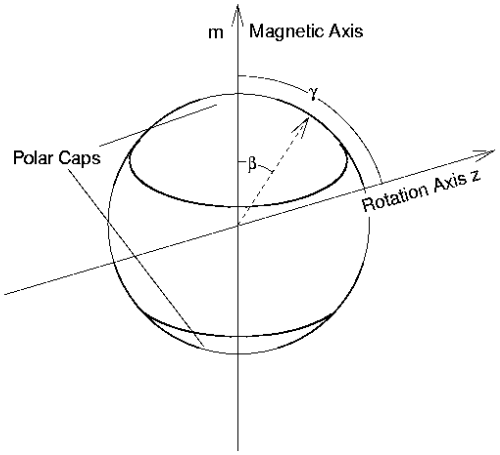

Fig. 3. Main geometrical parameters used in our model: γ is the angle between the magnetic and the rotation axis. β defines the latitude of the polar caps.

4. Model and interpretation

In the context of the model described above, the intensity of the emission line depends upon 1) temperature of the cyclotron-emitting plasma 2) emitting fraction of the star surface. The range of the dipole field spanned by the emitting plasma surface determines the frequency width of the observed feature. Clearly, the ion gyrofrequency formula allows us to determine the value of the star' s magnetic field as a function of the frequency of the observed line. Since the ratio A/Z (which defines the chemical composition and the ionization level of the emitting atmosphere) is unknown, the magnetic field value is, in principle, determined only within a factor of ~ 2. On the other hand, our model yields a clear prediction of a sharp intensity decrease at the frequency value corresponding to the B field maximum, located close to the magnetic poles. To compute a B field value, the emitting medium is assumed to be either H or He, yielding a well-defined A/Z ratio. This is consistent with the strong stratification of the elements induced by the huge gravitational field of the neutron star. Hydrogen and Helium differ by a factor two in their ratio A/Z, so that the cyclotron second harmonic of the heavier element overlaps exactly the fundamental one of the lighter. The position of the polar caps with respect to the star magnetic axis is shown in Fig. 3. The polar cap extension, given by the angle β, determines the frequency width of the cyclotron emission. The magnetic axis forms an angle γ with the rotation axis. The model will be fully determined once the angle, α, between the observer and the rotation axis, is defined (see

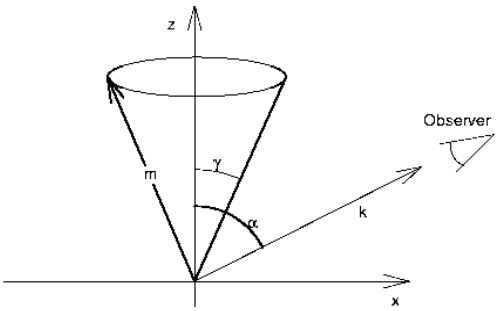

Fig. 4. Apart from γ and β, our model call for a third angle, α, between the wave vector, pointing toward the observer, and the rotation axis. The γ angle between the magnetic and the rotation axis is also shown.

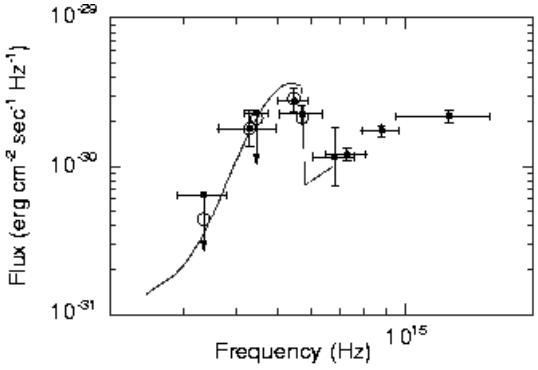

Fig. 5. Radiation flux ($erg\ cm^2\ s^{-1} Hz^{-1}$) versus frequency (Hz) in the region near the cyclotron resonance frequency. The data of Fig. 1 (close symbols) are compared with the the ion cyclotron emission computed on the basis of our model (solid line). In order to make the curve immediately comparable to the data points, we have filtered the curve through the passbands actually used in the photometric observations. The resulting fluxes are shown as open symbols.

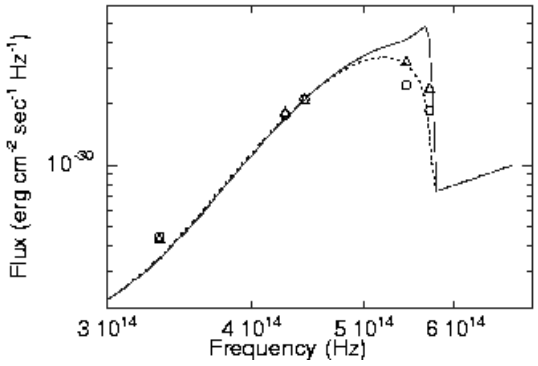

Fig. 6. Prediction of the model under the assumption of the oblique rotation geometry ($\gamma = 90$) and for α close to 20°. Both the line intensities (triangles and circles refer to the maximum and minimum emission respectively) and profiles (solid and dotted lines) are seen to vary with the rotation phase.

Fig. 4). Fig. 5 compares the data (filled circles) to the cyclotron emission model (open circles). The thin continous line shows the detailed shape of the feature as determined by the model. The open circles are obtained by integrating the model data over the filter passbands. The computed magnetic field ranges from $3.8\,10^{11}\ G$ for the case of a pure Hydrogen plasma to $7.6\,10^{11} G$ in the case of Helium. The model data shown in Fig. 5 have been obtained with the following assumptions: magnetic pole plasma temperature $T_0 = 9\,10^7\,^\circ K$; temperature profile along the polar caps assumed to be gaussian-like $T = T_0 exp[-(\beta/\beta_0)^4]$ with $\beta_0 = 57^\circ$. With this choice of parameters the plasma temperature drops to 1/10 of its maximum value in about 60°. Such an extension of the plasma polar caps is required to explain the width of the line. Of course, the observed line intensity and the plasma temperature are also determined by Geminga's radius and by its distance from the observer. We assumed a radius $r_0 = 10\ km$ and the parallax distance of 157 pc. Reasonable geometry uncertainties, however, do not change the order of magnitude of the plasma temperature required to emit such an intense cyclotron line. Fig. 6 gives a prediction of our model under the assumption of the oblique rotation geometry ($\gamma = 90^\circ$) and for α close to 20°, both the line intensities and profiles are seen to vary with the rotation phase. For this choice of parameters the modulation factor is about 15% and the profile is seen to sharpen close to the emission maximum (i.e. when the $\boldsymbol{B}$ axis sweeps over the observer direction). Obviously, the region around 5500 Å should be the ideal one for observing the feature modulation and profile.

5. Electron cyclotron emission and absorption

Geminga's polar cap atmosphere has been modelled as a fully ionized gas with a density $\simeq 10^{19} cm^{-3}$ and temperature $\simeq 9\,10^7\,^\circ K$. The associated electron-ion energy equipartion time, under these model assumptions, keeps ions and electrons close in temperature. The electron cyclotron emission process is thus quite efficient and the electron cyclotron line, associated to the companion ion cyclotron line, is expected to be an observable feature. This is in contradiction with the experimental data (see the combined ROSAT/ASCA X-ray spectrum) that show no line feature at E=4 or 8 keV i.e. in the X-rays spectral range where the electron spectral line should fall. A possible explanation based on the observation that, within a blackbody emission approximation, the power emitted at the electron cyclotron frequency is so high that the rate of relaxation between parallel and perpendicular (to the magnetic field) temperature is not sufficient to keep the electron distribution function isotropic (Ichimaru 1973; Trubnikov 1965). The anisotropy of the electron distribution function, following this line of thought, would then reach a steady state when the cyclotron emitted power, which is proportional to the perpendicular temperature (Bornatici et al. 1983), is lower than the one predicted by the isotropic case.

In order to give a quantitative estimate of the steady state anisotropy and emission a kinetic calculation is required by means of a relativistic Fokker-Planck equation which includes a quasilinear term of interaction with electron cyclotron radiation. This is, at present, beyond the target of this work.

A possible explanation of the fact that the residual emission is not observed is given by the polar cap heating model proposed for Geminga by Halpern & Ruderman (1993). Following this model a flux of e^+e^- pairs is created on closed field lines

lying outside the star and channelled into the polar caps of Geminga with a residual energy of about 6.5 erg each (Halpern & Ruderman 1993). The $e^{\pm}$ cloud embedded in the dipole magnetic field, which decreases by increasing the distance from the star surface, can thus act as a "second harmonic" resonant absorber of cyclotron radiation emitted from regions closer to the star surface. The resonant radial position is located at $r_{2nd} = 2^{1/3} r_0$, and, owing to the electron cyclotron line width $\Delta\omega/\omega_{ce} = v_{the}/c$ (where ω_{ce} is the angular frequency of the electron cyclotron emission and v_{the} the thermal velocity of the electrons) extends over about 300 m. It can be shown (Bornatici et al. 1983) that the E=4 keV line is efficiently absorbed ("optical depth" $\tau \simeq 16$) by the $e^{\pm}$ cloud, providing that $(n_{\pm} T_{\pm}) \simeq 100$ where $n_{\pm}$ and $T_{\pm}$ are density and temperature of $e^{\pm}$ respectively ($n_{\pm}$ in 10^{15} units and $T_{\pm}$ in keV). Typical densities $n_{\pm} \simeq 10^{17}\, cm^{-3}$, corresponding to column densities $\simeq 10^{22} cm^{-2}$, with a temperature of $\simeq 2\ 10^6\ ^\circ K$ (0.2 keV), for instance, will attenuate the electron cyclotron line by a factor $\simeq 10^7$. The electron cyclotron emission, following these model assumptions, can no longer be observed as a spectral feature.

6. Conclusions

The data shown in Fig. 1 leave no room for doubt that a wide emission feature exists in the optical region of Geminga's thermal continuum. The feature falls in the wavelength region where the atmospheric ion-cyclotron emission will be located close to the surface of a magnetic neutron star. Since Geminga is a magnetic neutron star, to wit its periodic γ-ray emission, and most probably has an atmosphere, to wit its soft X-ray emission, we have provided here a semi-quantitative interpretation for such feature. It is based on the reasonable assumption that the polar cap regions of the NS are covered by a thin plasma layer heated to a temperature higher that the global surface atmosphere by, e.g., infalling particles. This is not a new scenario per se. It was foreseen both in the case of INS accretion of ionized matter funnelled towards the poles by the B-field configuration and of magnetospheric particles drawn back to the polar surface by the strong E field induced by the oblique rotator.

The plausibility of this emission model in the visible range frequencies is also supported by estimate of power balance performed along the line proposed by Halpern & Ruderman. In the case of Geminga a pair flux in excess of $\dot{N} = 10^{38} s^{-1}$ can release in the emitting plasma layer a linear power density $\dot{N} dE/dr \simeq 10^{28}\, erg\ cm^{-1} s^{-1}$ (Jackson 1975). This power is sufficient to compensate plasma losses mainly due to the ion cyclotron emission and Bremsstrahlung over the whole star surface.

What is new here is the excellent fit obtained to the multiple experimental data by our physical model using a minimum of assumption. In particular, we have shown that the feature could not originate over the whole star surface, because global B-field variations would induce a feature wider than observed. The only free parameter is the geometry of the emission with respect to the observer; note, however, that our geometry is fully compatible with the oblique rotator proposed for Geminga by Halpern & Ruderman (1993). The assumption that the composition of the outer emitting layer is either H or a light, fully ionized element mixture is supported by the estimated value for the magnetic field. Such a value is in good agreement with the standard pulsar magnetic field prediction. It represents, in fact, the first independent measurement of the surface magnetic field of an INS.

Acknowledgements. Useful discussions with Prof. Bruno Bertotti are gratefully acknowledged.

References

Akhiezer A.I., Akhiezer A., Polovni R.V., Sitenko A.G., Stepanov K.N., 1975, Plasma Electrodynamics. Vol.I, Pergamon Press
Becker W., Trümper J., 1997, A&A 326, 682
Bekefi G. 1966, Radiation Processes in Plasmas. John Wiley & Sons, New York
Bignami G.F., Caraveo P.A., 1996, ARA&A 34, 331
Bignami G.F., Caraveo P.A., Mignani R., Edelstein J., Bowyer S., 1996, ApJ 456, L111
Bornatici M., Cano R., De Barbieri O., Engelmann F., 1983, Nuclear Fusion 23, 1153
Caraveo P.A., Bignami G.F, Mignani R., Taff L., 1996, ApJ 461, L91
Caraveo P.A., 1998, Adv. in Space Research Vol. 21 n.1/2, 187
Gull T.R., et al., 1998, ApJ 495, L51
Halpern J.P., Ruderman M.R., 1993, ApJ 415, 286
Halpern J.P., Wang F.Y., 1997, ApJ 477,905
Hill R.J., et al., 1997, ApJ 486, L99
Ichimaru S., 1973, In: Basic Principles of Plasma Physics. A Statistical approach. W.A. Benjamin Inc., Reading, Massachussetts, USA
Jackson J.D., 1975, Classical Electrodynamics. 3rd ed., Wiley, New York, Chap. 13
Martin C., Halpern J.P., Schiminovich, D., 1998, ApJ 494, 211
Meyer E.D., Pavlov G.G., Meszaros P., 1994, ApJ 433, 265
Mignani R., Caraveo P.A., Bignami G.F., 1998, A&A 332, L37
Nasuti F.P., Mignani R., Caraveo P.A., Bignami G.F., 1996, A&A 314, 849
Romani R.W., 1987, ApJ 313, 718
Shafranov V.D., 1958, In: Coll.: Plasma Physics and Problems of Controlled Thermonuclear Reactions. Moscow, Akad. Navk. SSSR, 1960, Oxford, Pergamon Press 4, 416
Shearer A., Golden A., Harfst F., et al., 1998, A&A 335, L21
Trubnikov B.A., In: Reviews of Plasma Physics, edited by M.A. Leontovich (Consultants Bureau, New York, 1979), Vol 7, p. 345